A-ph 1801.03501

Probing star formation and ISM properties using galaxy disk inclination I

Evolution in disk opacity since $z \sim 0.7$

S. K. Leslie[1⋆], M. T. Sargent[2], E. Schinnerer[1], B. Groves[3], A. van der Wel[1], G. Zamorani[4], Y. Fudamoto[5], P. Lang[1], and V. Smolčić[6]

[1] Max-Planck-Institut für Astronomie, Königstuhl 17, 69117, Heidelberg, Germany
[2] Astronomy Centre, Department of Physics and Astronomy, University of Sussex, Brighton BN1 9QH, UK
[3] Research School of Astronomy and Astrophysics, Australian National University, Canberra, ACT 2611, Australia
[4] INAF-Osservatorio Astronomico di Bologna, via Gobetti 93/3, 40129, Bologna, Italy
[5] Observatoire de Genéve, 51 Ch. des Maillettes, 1290 Versoix, Switzerland
[6] Faculty of Science University of Zagreb Bijenička c. 32, 10002 Zagreb, Croatia
e-mail: leslie@mpia.de

January 12, 2018

ABSTRACT

Disk galaxies at intermediate redshift ($z \sim 0.7$) have been found in previous work to display more optically thick behaviour than their local counterparts in the rest-frame B-band surface brightness, suggesting an evolution in dust properties over the past ~6 Gyr. We compare the measured luminosities of face-on and edge-on star-forming galaxies at different wavelengths (Ultraviolet (UV), mid-infrared (MIR), far-infrared (FIR), and radio) for two well-matched samples of disk-dominated galaxies: a local Sloan Digital Sky Survey (SDSS)-selected sample at $z \sim 0.07$ and a sample of disks at $z \sim 0.7$ drawn from Cosmic Evolution Survey (COSMOS). We have derived correction factors to account for the inclination dependence of the parameters used for sample selection. We find that typical galaxies are transparent at MIR wavelengths at both redshifts, and that the FIR and radio emission is also transparent as expected. However, reduced sensitivity at these wavelengths limits our analysis; we cannot rule out opacity in the FIR or radio. Ultra-violet attenuation has increased between $z \sim 0$ and $z \sim 0.7$, with the $z \sim 0.7$ sample being a factor of ~3.4 more attenuated. The larger UV attenuation at $z \sim 0.7$ can be explained by more clumpy dust around nascent star-forming regions. There is good agreement between the fitted evolution of the normalisation of the SFR_{UV} versus 1-cos(i) trend (interpreted as the clumpiness fraction) and the molecular gas fraction/dust fraction evolution of galaxies found out to $z < 1$.

To study the inclination dependence of attenuation, we must rely on samples of galaxies that differ only in their viewing angle (Devour & Bell 2016). To achieve a sample of such galaxies both locally and at intermediate redshift ($z \sim 0.7$), we select galaxies from the SDSS and COSMOS survey regions of the sky, respectively.

At both $z \sim 0$ and $z \sim 0.7$ we selected star-forming galaxies with stellar masses $\log(M_*/\mathrm{M}_\odot) > 10.2$, g-band half-light radii $r_{1/2}$ >5 kpc, and Sérsic index n <1.2. These cuts were made to minimise selection biases whilst maintaining a reasonable number of galaxies in our $z \sim 0.7$ sample and will be discussed in more detail in the following sub-sections.

$$\cos^2(i) = \frac{(b/a)^2 - (b/a)^2_{\mathrm{min}}}{1 - (b/a)^2_{\mathrm{min}}},$$

Table 1. Data used for SFR estimation. The area Ω quoted is the overlap between the particular wavelength and the SDSS or ACS surveys from which the morphological parameters are drawn. N_{gals} is the number of galaxies in our sample detected at each wavelength with robust mass, inclination, and SFR measurements (Signal-to-noise ratio (S/N)>3).

Wavelength	Instrument	Survey	Ω (deg^2)	3σ (μJy)	N_{gals}	References
COSMOS UV	GALEX (NUV)	DIS	1.7	0.23	296	(1)
COSMOS MIR	Spitzer MIPS (24μm)	S-COSMOS	1.7	43	373	(2,3)
COSMOS FIR	Herschel PACS (100μm)	PEP	1.7	5000	87	(4,5)
COSMOS Radio	VLA (S-band, 3GHz)	VLA-COSMOS 3GHz	1.7	7	58	(6,7)
SDSS UV	GALEX (FUV)	MIS	~1000	1.8	788	(8)
SDSS MIR	WISE (W3, 12μm)	AllWISE	~8400	340	6008	(9,10)
SDSS FIR	IRAS (60μm)	FSC	~8400	1.2×10^5	80	(11)
SDSS Radio	VLA (L-band, 1.4GHz)	FIRST, NVSS	~8400	450	58	(12,13,14)

References. (1) Capak et al. (2007); (2)Sanders et al. (2007); (3)Le Floc'h et al. (2009); (4)Poglitsch et al. (2010); (5)Lutz et al. (2011); (6)Smolčić et al. (2017a); (7)Smolčić et al. (2017b); (8)Bianchi et al. (2011); (9)Wright et al. (2010); (10)Chang et al. (2015); (11)Moshir & et al. (1990); (12)Kimball & Ivezic (2014); (13)Becker et al. (1995); (14)Condon et al. (1998).

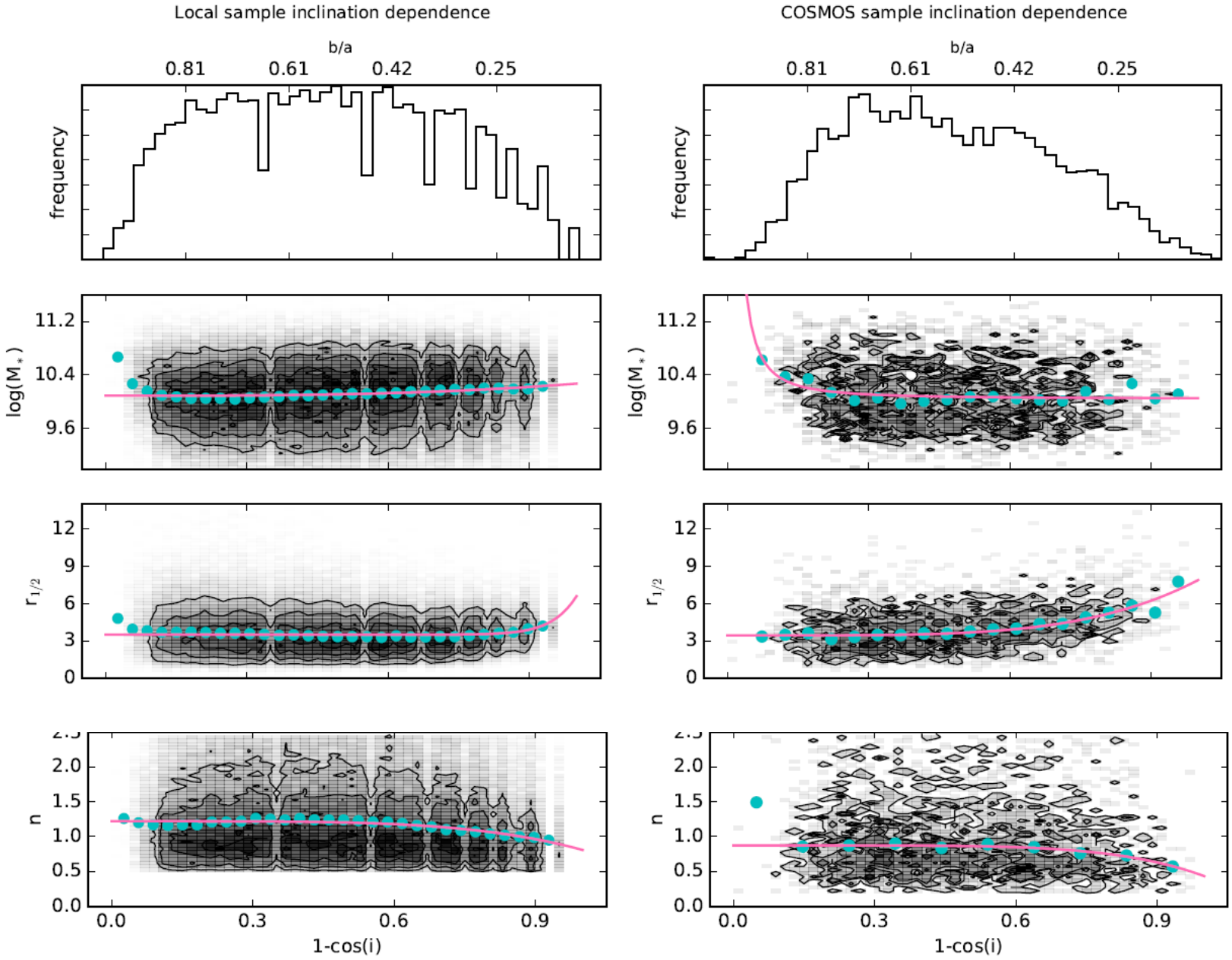
Local sample inclination dependence
COSMOS sample inclination dependence
b/a
0.81
0.61
0.42
0.25
frequency
log(M*)
11.2
10.4
9.6
r1/2
12
9
6
3
0
n
2.5
2.0
1.5
1.0
0.5
0.0
0.0
0.3
0.6
0.9
1-cos(i)

Как оценивалась SFR?

We use the SFR calibration derived for the GALEX FUV bandpass to calculate SFR_{UV} for our local sample. No correction for dust attenuation is applied.

For both the mid- and far-IR monochromatic tracers, we convert the monochromatic flux density to the total infrared luminosity (8-1000 m) using the Wuyts et al. (2008) spectral energy distribution (SED) template and then calculate the SFR using the

- LIR calibration of Murphy et al. (2011).

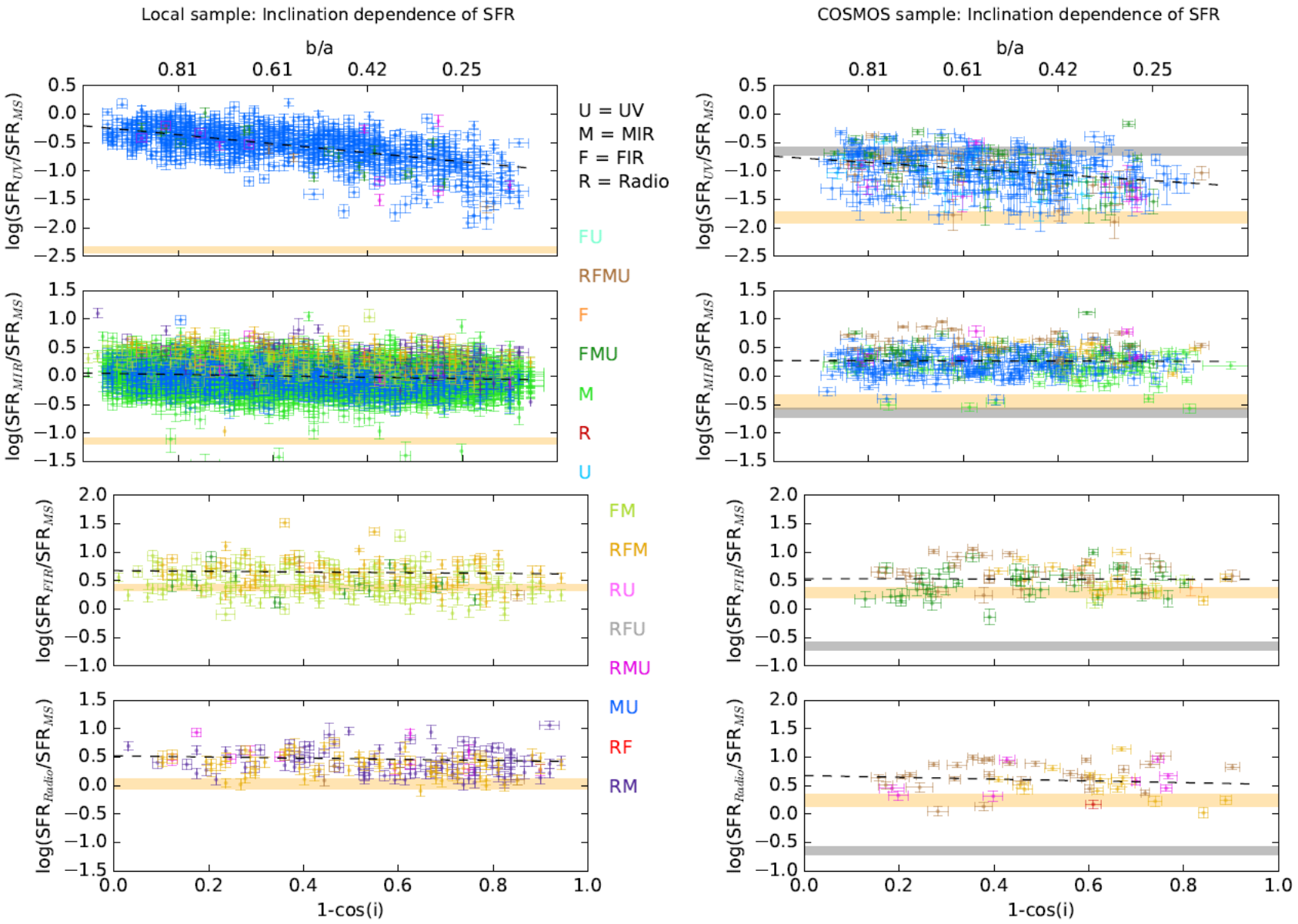

Fig. 3. Inclination dependence of multiwavelength SFRs. y-axis: $\log(\mathrm{SFR}_\lambda)$ - $\log(\mathrm{SFR}_{\mathrm{MS}})$. Top to bottom shows UV, MIR, FIR, and radio-determined SFR. x-axis: 1-cos(i), where i is the galaxy inclination. Face-on galaxies are on the left of the plot (at 0) and edge-on galaxies are on the right-hand side (at 1). The left panels show SDSS galaxies ($0.04 < z < 0.1$) and the right panels show COSMOS galaxies ($0.6 < z < 0.8$).

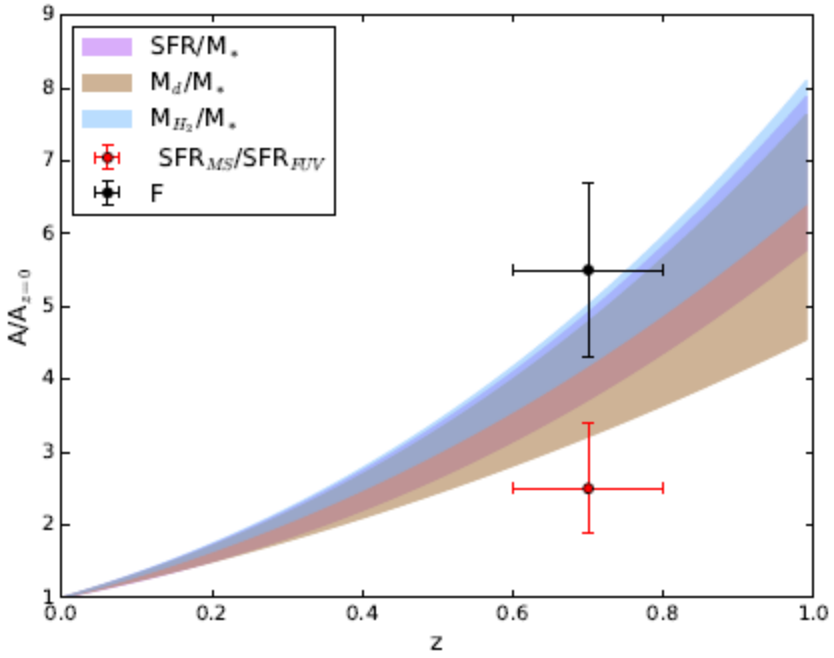

Fig. 8. Evolution of massive galaxy properties from their local values out to $z \sim 1$. The evolution of the dust-mass fraction (M_d/M_*) was determined from a power-law fit to data from Santini et al. (2014), Béthermin et al. (2015) (for $z \leq 1$), and Rémy-Ruyer et al. (2014) for $z = 0$. The upper bound to the M_d/M_* evolution is given by assuming $M_d \sim 0.5 \times Z \times M_g$, and the evolution of gas and metallicity over this redshift and stellar mass range. The evolution of specific SFR is shaded purple between the relationship in Sargent et al. (2014) and $(1 + z)^3$. The evolution of the molecular gas fraction (blue) is from Tacconi et al. (2017). We find that the fraction (F) of dust in clumps surrounding nascent star-forming regions has increased by a factor of ~6, and that the overall attenuation of UV (SFR_{MS}/SFR_{UV}) has increased by a factor of ~2.5 (ranging from 3.4 to 1.9 for face-on to edge-on galaxies, respectively).

Выводы

The FUV SFR of face-on galaxies at z = 0.7 is less than that expected from the main-sequence relation by a factor of 0.77pm0.09 dex, compared to 0.24pm0.03 dex at z = 0. This corresponds to an increase of the FUV attenuation of face-on galaxies by a factor 3.4 over the last 7.5 Gyr. An increased fraction of dust in warm clumpy components surrounding the HII regions (by a factor of about 6) could explain this increased overall attenuation.

This increase in the warm clump component and UV attenuation between z = 0 and z =0.7 is consistent with the increased molecular gas content in galaxies at redshift 0.7. Overall FUV attenuation increases with stellar mass surface density at both z 0 and z =0.7.

It is likely that no opacity is present in the FIR and radio. MIR and radio SFRs are inclination independent and therefore MIR and radio data can

provide a useful tracer of SFRs also for galaxies with a high inclination

angle.

A-ph 1801.01427

GAIA DR1 COMPLETENESS WITHIN 250 PC AND STAR FORMATION HISTORY OF THE SOLAR NEIGHBOURHOOD

Edouard J. Bernard[1]

Abstract. Taking advantage of the *Gaia* DR1, we combined TGAS parallaxes with the *Tycho-2* and APASS photometry to calculate the star formation history (SFH) of the solar neighbourhood within 250 pc using the colour-magnitude diagram fitting technique. Our dynamically-evolved SFH is in excellent agreement with that calculated from the *Hipparcos* catalogue within 80 pc of the Sun, showing an enhanced star formation rate (SFR) in the past ∼4 Gyr. We then correct the SFR for the disc thickening with age to obtain a SFR that is representative of the whole solar cylinder, and show that even with an extreme correction our results are not consistent with an exponentially decreasing SFR as found by recent studies. Finally, we discuss how this technique can be applied out to ∼5 kpc thanks to the next *Gaia* data releases, which will allow us to quantify the SFH of the thin disc, thick disc and halo *in situ*.

- The main advantages of the CMD-fitting technique over other methods of recovering the SFH (e.g. chemical enrichment models, colour-function fitting, age/metallicity census of individual stars, ...)are the fact that determining the age of a population is much more robust than that of single stars, that one takes full advantage of the predictions of stellar evolution models, and the smaller number of assumptions. On the other hand, like other methods it is affected by the systematic effects due to uncertainties in the stellar models, as well as the poorly constrained amplitude of radial migrations in the disc.

- While TGAS provides accurate parallaxes and G-band magnitudes for over 2 million stars, no colour information is available. On the other hand, the Tycho-2 catalogue does include BT, VT for all TGAS stars. We thus cross-matched TGAS with the Tycho-2, Hipparcos, and APASS DR9 (Henden et al. 2012) catalogues.
- The synthetic CMD from which we extracted the simple stellar populations' CMDs is based on the BaSTI stellar evolution library (Pietrinferni et al. 2004). It contains 2 10^7 stars and was generated with a constant SFR over wide ranges of age and metallicity: 0 to 15 Gyr old and $0.0001 < Z < 0.03$

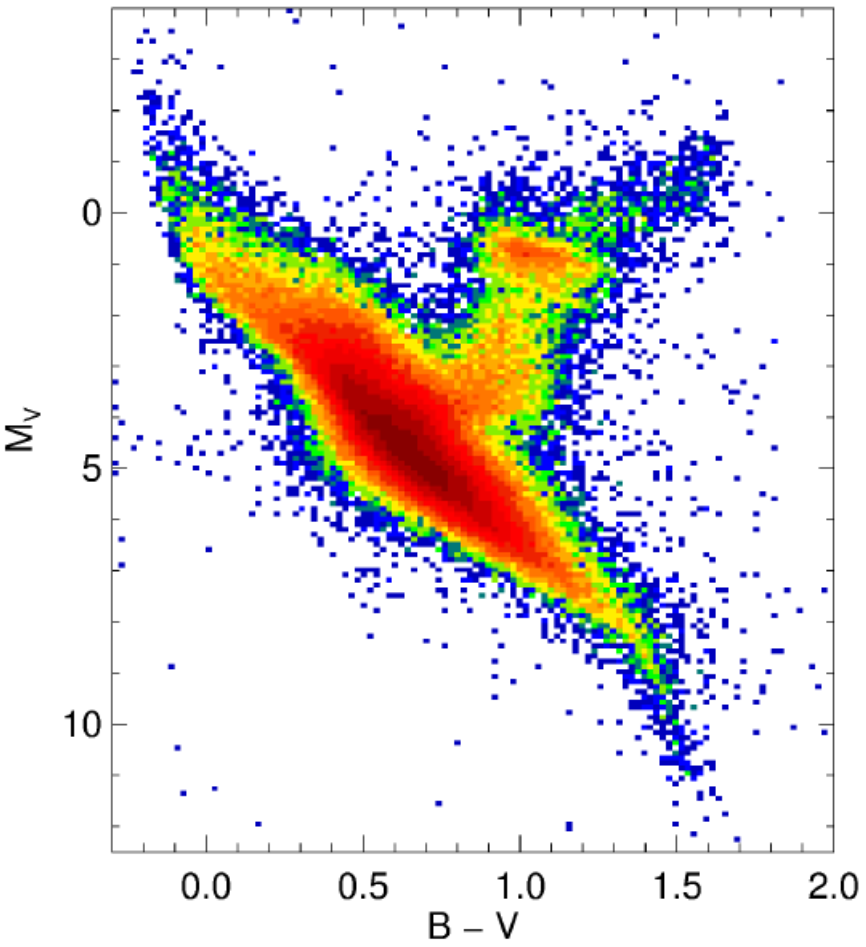

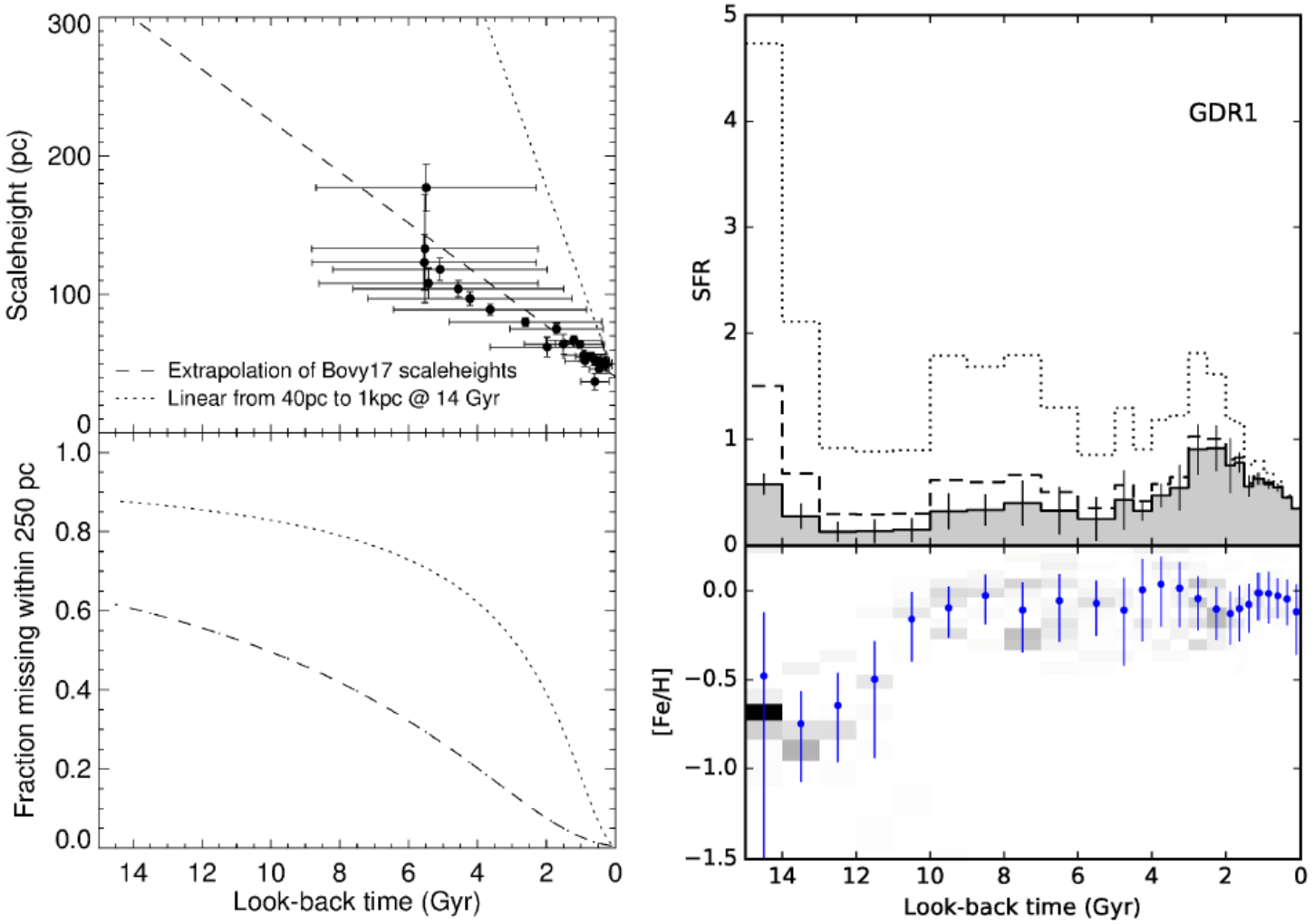

Fig. 2. Left: Evolution with time of the disc scaleheight (top) and of the corresponding fraction of stars lying beyond 250 pc (bottom, see text for details). The dashed and dotted lines correspond to the mild and the extreme corrections respectively. Right: Resulting SFH, showing the evolution of the SFR (top) and metallicity (bottom) as a function of time. In the top panel, the dashed and dotted lines represent the SFR corrected for the fraction of stars that have been heated to heights >250 pc, assuming the mild and the extreme corrections respectively.

Основной вывод

- We correct SFR for the disc thickening with age to obtain a SFR that is representative of the whole solar cylinder, and show that even with an extreme correction our results are not consistent with an exponentially decreasing SFR.

We plan to use the same technique with upcoming Gaia data releases. With parallaxes and homogeneous photometry in 3 bands (G, BP, RP) for $>10^9$ stars, and it will allow us to extend this analysis out to about 5 kpc, and therefore to quantify the SFH of the thin disc, thick disc and halo..

A-ph 1801.03020

Spiegel Lubov* and Polyachenko Evgeny

- **Multiarm spirals on the periphery of disc galaxies**

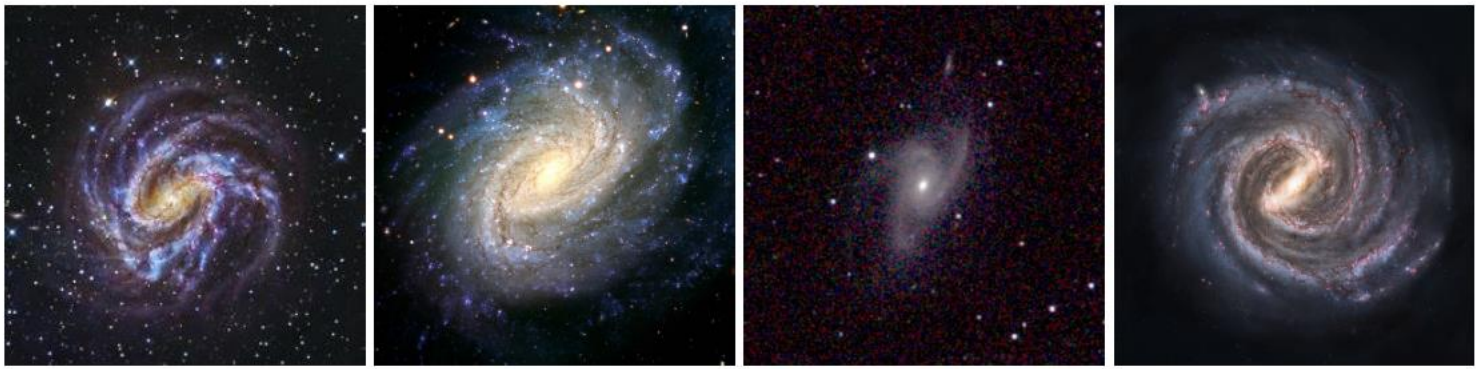

Fig. 1. Examples of disc galaxies with three or more peripheral arms (from the left): M83 (RGB, Anglo-Australian Observatory), NGC 1187 (BV, VLT), NGC 5054 (JHK, 2MASS), 'Milky Way' (reconstruction).

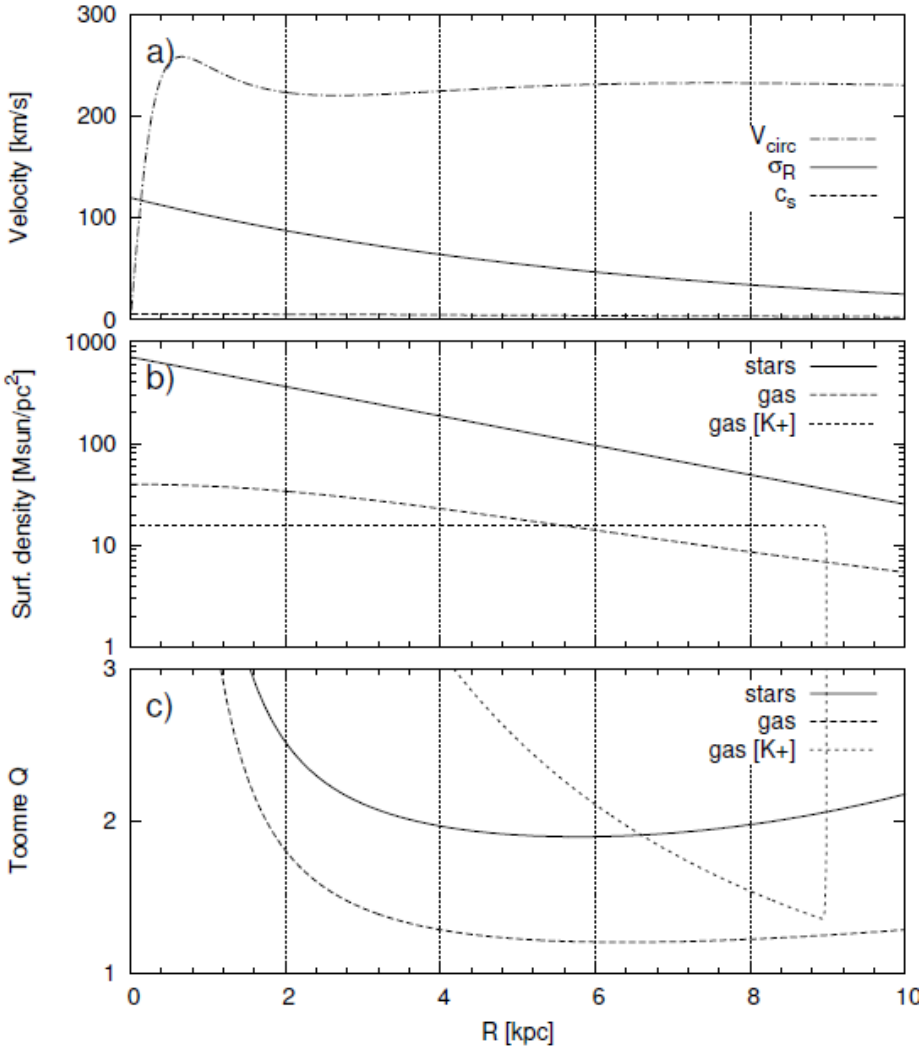

Fig. 2. The Galaxy model profiles: a) the rotation curve $V_{\rm circ}(R)$, the radial dispersion of the velocities of the stars $\sigma_R(R)$ and the turbulent sound speed $c_{\rm s}(R)$; b) the surface density of the stellar and gaseous discs; c) Toomre parameters(7) for stellar and gaseous discs. In panels b) and c) the short dashes show the corresponding profiles for the gaseous disc for the initial parameters adopted in K+.

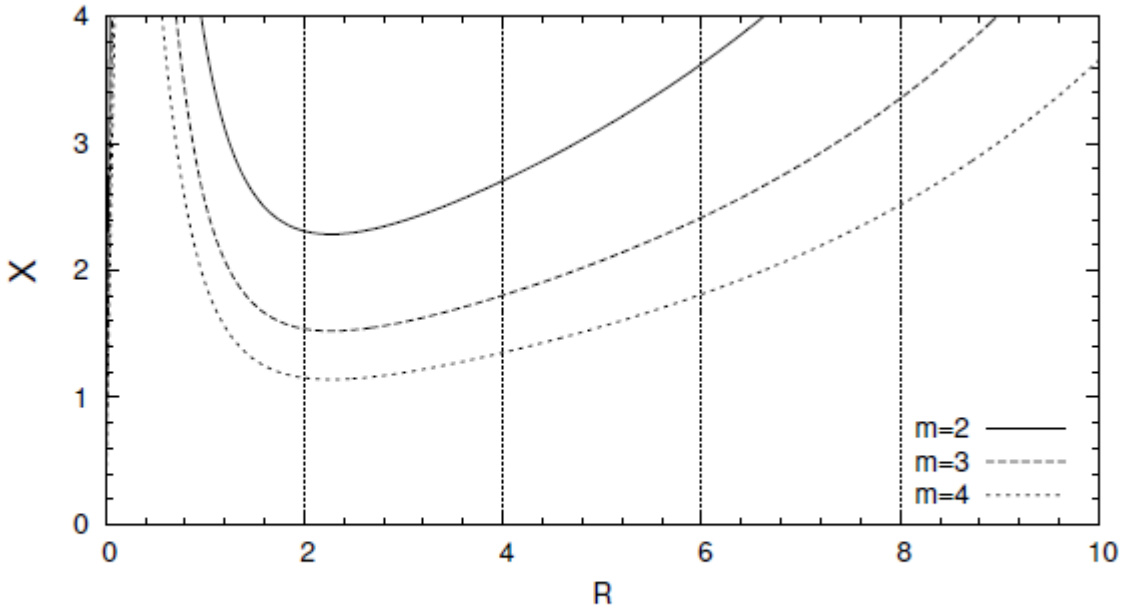

Fig. 5. The profiles $X(R)$ for $m = 2, 3, 4$.

$$X \equiv \lambda_\theta / \lambda_{\rm crit} \ ,$$

$$\lambda_\theta = 2\pi/k_\theta = 2\pi R/m, \ \lambda_{\rm crit} = 4\pi^2 G\Sigma_0/\kappa^2.$$

Вывод

- We suggest that three-arm spirals can be explained by the rapid cooling of the gas component, which is accompanied by the appearance of molecular clouds. The latter, in turn, induce multi-arm spirals through the swing amplification mechanism.

As follows from the graphs of Toomre stability parameter Q and $Q_{\rm g}$, the initial value of the turbulent sound speed equal to 8 km/s, turn very quickly to 4 km/s at a radius $R = 5\,\mathrm{kpc}$. The needed cooling for the scenario described above is 3 km/s. We believe that this is quite realistic. In the future, we plan to test our hypothesis for multi-arm spiral formation using N-body simulations.

Оценка параметра Q для галактик THINGS на $R=R_{25}$ с использованием новых оценок дисперсии скоростей HI (по lanjamasimanana et al ,2015)

1	*2*	*3*	*4*
NGC	R_{25}, кпк	σ_V, км/с	Q
NGC925	14.3	8.8	1.8
NGC2366	2.2	11.3	3.1
NGC2403	7.4	8.4	2.9
NGC2903	15.2	9.9	4.3
NGC2976	3.8	9.6	13.8
NGC3198	12.9	12.5	2.8
IC2574	7.5	8.1	1.5
NGC3621	9.4	10.0	3.3
NGC4736	5.3	7.7	10.4
DDO154	1.2	8.7	2.4
NGC5055	17.2	8.9	3.5
NGC6946	9.8	7.7	4.6
NGC7793	5.9	9.6	2.3